Theoretical and gas-phase studies of specific cationized purine base quartet.

Sakina Mezzache, Sandra Alvès, Jean-Paul Paumard, Claude Pepe, Jean-Claude Tabet

Theoretical and gas-phase studies of specific cationized purine base quartet

Sakina Mezzache[1], *Sandra Alves*[1], *Jean-Paul Pommard*[2], *Claude Pepe*[2*], *Jean-Claude Tabet*[1]

[1]Université Pierre et Marie Curie-Paris 6; CNRS. Synthèse, Structure et Fonction de Molécules Bioactives, UMR 7613, 4 place Jussieu, 75252 Cedex Paris, France.

[2]Université Pierre et Marie Curie-Paris 6; CNRS. Laboratoire Dynamique Interactions et Réactivité, UMR 7075, case 49, 4 place Jussieu, 75252 Cedex Paris, France.

*Author for correspondence

Phone number: (33) 1 44 27 30 74

Fax number: (33) 1 44 27 30 21

e-mail: pepe@ccr.jussieu.fr

Running title : Studies of specific cationized purine base quartet

Abstract: Guanine tetraplexes are biological non-covalent systems stabilized by alkali cations. Thus, self-clustering of guanine, xanthine and hypoxanthine with alkali cations (Na^+, K^+ and Li^+) is investigated by electrospray mass spectrometry (ESI-MS) in order to provide new insights of G-quartets, an hydrogen bonded complexes. Electrospray ionization assays displayed magic numbers of tetramer adducts with Na^+, K^+ and Li^+, not only for guanine but also for xanthine bases. The optimised structures of guanine and xanthine quartets have been determined by B3LYP hybrid density functional calculations. Complexes of metal ions with quartets are classified into different structure types. The optimised structures obtained for each quartet explain the gas phase results. The gas-phase binding sequence between the monovalent cations and the xanthine quartet follows the order $Li^+ > Na^+ > K^+$, which is consistent with that obtained for guanine quartet in the literature. The smallest stabilization energy of K^+ and the geometric distorsion versus the other alkali metal ions in guanine and xanthine quartets is consistent with the fact that the potassium cation can be located between two guanine or xanthine quartets, for providing a [gua (or $(xan)_8$) + K]$^+$ octamer adduct. Even if, an abundant octamer adduct with K^+ for xanthine was detected by ESI-MS, it was not the case for the guanine.

Keywords: cluster ions, G-quartet, ESI ionization, DFT calculation, cations.

INTRODUCTION

Among the five nucleobases constituting the building blocks of DNA strand, the guanine base is unique as containing both hydrogen donating and neighboring hydrogen accepting groups. Thus, it can form a self-complementary hydrogen bonding tetramer. The tetrameric forms of guanine, known as G-quartets (in DNA), are implied in a variety of biological functions. It was found that they exist in telomere[1] DNA (in human sequence), which consists of several kilobases of repeated $(TTAGGG)_n$ sequences at the ends of linear chromosomes. Human telomerase, which is a ribonucleoprotein, is the enzyme allowing the stabilisation of telomeres by adding TTAGGG repeats to telomere ends. The invariance of telomere length is essential for cell survival. In about 85% of tumors; the enzyme telomerase is active. It maintains telomeres length in cancer cells and ensures the cells immortality that is their ability to reproduce without limit. Hence the increased interest[2,3] in the anticancer potential of compounds that bind G-quadruplexes selectively, thus stabilizing them and potentially disabling telomerase. The G-quadruplex-cancer relation is based upon the notion that single-stranded telomeric DNA must be linear and unfolded to allow telomerase to catalyse telomere extension and that G-quadruplex folding prevents the enzyme from carrying out this function. Solution-phase studies of G-quadruplexes have shown that cations such as K^+, Na^+ and NH_4^+ bind G-quadruplexes, stabilize them and inhibit telomerase activity[4]. Because of their importance, G-quartets in the presence of monovalent cations have been investigated by several techniques using X-ray[5], gel eletrophoresis[6], scanning probe microscopy[7], circular dichroism[8] and NMR[9,10,11,12]. Quantum calculations have revealed that cation-guanine-quartet complexes adopt the normal four-stranded Hoogsteen-bonded G-quartet structure[13,14] (Figure 1b). The binding sequence, determined by calculations, between the alkali cations and the G-quartet complexes which follows the order $Li^+ > Na^+ > K^+$, is in contrast to the stabilizing order in aqueous solution $K^+ > Na^+ > Li^+$[15].

In order to establish the intrinsic chemical properties of cationized G-quartert in the absence of any external factors such as solvent, salt presence and pH, these systems can be investigated in the gas phase by using mass spectrometry, mainly electrospray ionization[16] (ESI) which is known to be useful for the study of the noncovalent interaction of biomolecules[17], by partially preserving their native conformation. In fact, specific interactions have been observed in the gas phase under special experimental conditions[18,19] and ESI data showed good correlations with solution phase behavior[20]. Several papers[21,22] have reported the observation of gas

phase G-quadruplexes by ESI. In order to provide various insights into the gas-phase conformation of the G-quadruplex with salts, studies using ion mobility[23] and hydrogen/deuterium exchange[24] have been reported in the literature. Other studies have focused on smaller systems for providing more information on the conformation of G-quadruplex. Clustering of natural nucleobases with metal ions[25,26,27] has been shown to be dependant upon the function of the nucleobase' s nature or the cation[28]. In the gas phase, the guanine is known to form magic number quartet adducts with Na^+. Similarly, cation-nucleobases[25,27], cation-nucleosides[29,30] and cation-nucleotides[31] have also been studied by mass spectrometry. Even if gas phase equivalent of the aqueous guanine quartet was observed, observation of additional magic number clusters indicated that the interactions are not directly correlated with solution phase studies. Some clusters result from non-specific aggregations in the course of ESI processes, whereas others appear to be specific to the solution transferred into the gas phase[18,19].

In our study, clustering of purine bases such as guanine, xanthine and hypoxanthine (Figure 1a) in the presence of the alkali cations (lithium, sodium and potassium) was investigated by electrospray ionization mass spectrometry. This experiment was undertaken in order to elucidate a possible correlation occurring between cluster formation ability and base physico-chemical properties. Hypoxanthine and xanthine are not incorporated into the biological nucleic acids but these bases are important intermediates in the synthesis and degradation of the purine nucleotides[32]. Clustering of guanine was compared to that occurring with its purine derivates to enlighten the influence of hydrogen donating or acceptor groups present on purines[33]. High level theoretical calculations were done to complement the mass spectrometry experiments. As the computational demand increases with the molecule size, density functional theory is an attractive alternative for nucleic acids model systems[34]. We have used the B3LYP hybrid density functional method to analyse guanine and xanthine quartet structures with alkali ions.

EXPERIMENTAL SECTION

Chemicals: The compounds studied (Figure 1a) guanine, hypoxanthine, xanthine were purchased from Sigma Aldrich (Steinheim, Germany) and used without further purification. The chloride salts (lithium, sodium and potassium) and the solvents used were obtained from Sigma Alrdich (Steinheim, Germany).

Instrumentation: Cluster adducts were formed by electrospraying a solution mixture containing a 0.01 M nucleobase and alkali metals at 0.01 M, diluted in a mixture of CH_3OH/H_2O (1:1). Acidification of guanine solutions was done by addtion of 0.01 % volume of acetic acid solution. Note that guanine exhibits poor solubility. The solubility of the guanine aqueous solution was improved by sonication or incubation at 50°C. Experiments were conducted in positive ion mode using an ion trap mass spectrometer (ESQUIRE, Bruker, Bremen, Germany), equipped with an ESI ionisation source (Analytica of Brandford, CT, USA). The following source voltages were used: capillary -3500 V, end plate -2800 V, capillary exit +45 V, skimmer +10 V*,* the source temperature was set to 180 °C and low mass cut-off value of 110 Th was chosen. The solution was introduced into the ESI source at a flow rate of 2.5 $\mu L.min^{-1}$ using a syringe pump. The m/z range was 100-1500 Th (" *standard*" mode) with a resolution of 0.4 Th (width at half height of peak).

Computational method: The structures of guanine and xanthine quartets were determined by B3LYP hybrid density-functional method in conjunction with the valence bouble-ξ basis set augmented with d and p-like polarization functions 6-31G(d,p) to ensure a correct description of the H-bonded system. The B3LYP approach predicts reliable interaction energies and is compatible with the MP2 calculations. The number of basis functions in the studied systems varies, for example for the xanthine from 241 (for $[xan_4+Li]^+$) to 249 (for $[xan_4+K]^+$). Energy minima were verified with subsequent frequency calculations but the interaction energies were not corrected for the basis set superposition error (BSSE) with the standard counterpoise method because of the negligible values of the corrections (less than 5 $kJ.mol^{-1}$). All calculations were carried out with Gaussian 03[35].

RESULTS

Gas-phase experiments under ESI-MS conditions

The goal of this research is to gain insight on the self-aggregation of purine bases by employing electrospray (ESI) mass spectrometry. ESI ionisation is known to be useful for studying noncovalents complexes by transferring labile complexes from solution to gas-phase[17,18]. Although our experiments are not performed under physiological conditions, large cluster adduct ions are detected but their abundances are dependent upon the experimental conditions, mainly the solution conditions as well as the operating source conditions (as cone

voltage). Cluster formation increases with increasing base concentration. The larger abundances of multimer were reached after addition of 0.2 equivalent of chloride salts. The multimers gradually disappear by increasing the base to salt ratio. When one equivalent of salt solutions is added, only the unique nucleobase monomeric adduct signal is displayed. Guanine exhibits very poor solubility in acetonitrile, methanol, and water. Hence the difficulty to study its clusters with alkali ions by electrospray mass spectrometry. Cooks *et al.* studied the ESI-MS of the guanine clustering as a function of cations Na^+, K^+ and Li^+. Only, the guanine tetramer sodium adducts have been observed. Nevertheless, another study has shown that monovalent cations tested stabilize the tetramers of guanosine and deoxyguanosine which are more soluble in water. In our study, aqueous methanol is used to provide comparisons with the xanthine and hypoxanthine experiments. The solubility of the guanine aqueous solution was improved by sonication or incubation at 50°C. But, its poor solubility resulted in a lower total ion signal and higher background. The guanine base is studied by acidifying solutions or by adding alkali metals Na^+, K^+ and Li^+. The corresponding ESI mass spectra of guanine are compared to those of xanthine and hypoxanthine analogs. Theses latter bases, which are more soluble in water, are close structurally to guanine (Figure 1a). Table 1 summarizes the results displayed in the mass spectra when salts are added to the purines. In this way, normalized abundances of mono and multimeric adduct ions are reported for each experiment.

Guanine. The positive ESI mass spectrum of acidified guanine solution shows the fomation of a singly-protonated $[gua+H]^+$ monomer and $[gua_2+H]^+$ dimer (data not shown). Subsequently, we compare the clustering of guanine when transferred into the gas-phase in the presence of various alkali cations. Table 1 shows the formation of magic number cluster adducts of the guanine base after addition of chloride salts. The mass spectrum of guanine after addition of lithium chloride is dominated by both the lithiated guanine monomers and dimers, but an unexpected tetramer adduct is observed although no trimer adduct ions are detected. Above all, with both the sodium and potassium cations, a stable tetramer adduct ion is detected. The peak intensity ratios of tetramer adduct ions to monomer adduct ion are considerably higher for Na^+ and K^+ compared to Li^+ (Table 1). The larger abundance of the cationized tetramer relative to other cluster ions displayed in the mass spectra suggests that cationized tetramers have a unique structure characterized by an unsual stability. For example, in Figure 2a, a mass spectrum of guanine with K^+ shows that larger size cationized clusters $(gua_n+K)^+$ for $n \geq$

5 are not observed. The guanine clustering was compared with 2 purine analogs the hypoxanthine and xanthine.

Hypoxanthine. The structure of hypoxanthine depicted in Figure 1a makes it unable to form a self-complementary quartet. Actually, the ESI mass spectra (see Table 1) of hypoxanthine in the presence of alkali cations show mainly cationized monomer and abundant dimeric complexes. In sharp contrast to guanine, no magic number clusters were observed with alkali cations and hypoxanthine. The absence of larger cationized clusters indicates that no structure is favored by an especially stable association. These gas-phase observations are consistent with hypoxanthine structure. Additionnal experiments were done on xanthine base to shed light on the role played by the structural features of purine bases.

Xanthine. The mass spectrum of xanthine upon addition of lithium chloride solution mainly displays the formation of lithiated $[xan+Li]^+$ monomer and $[xan_2+Li]^+$ dimer adduct ions. Abundant cationized xanthine tetramers are observed with Na^+ and K^+, they represent characteristic magic number clusters in the ESI mass spectra. The extraordinary stability of the cationized tetramers, characterized by their high relative abundances in comparison to other clusters, makes the structure of these complex ions of great interest. The most intriguing finding is the formation of singly-charged octamer complex with only potassium cations (Figure 2b), which clearly represents a magic number clusters as no larger clusters $(xan_n+K)^+$ are observed for $5 \leq n < 8$.

Finally, the most important result of this experimental study is that unsualy stable tetramers are detected for guanine and xanthine by addition of alkali salts. Furthermore, an unexpected observation is the formation of a cationized octamer with K^+ for xanthine base. The propencity of both bases for clustering strongly suggests particular structural features and could be correlated to the existence of specific quartets and metaclusters. To understand how the different cations influence the observation of the complexes with alkali cations for xanthine and guanine, it is necessary to investigate their interactions with the quartet. One way to examine the change in host structure caused by the interaction of the cation can be the use of reliable theoretical calculations. Quantum calculations are then applied to the study of the guanine and xanthine quartet complexes. Theoretical studies were not undertaken on hypoxanthine base as no magic number cluster were observed by ESI experiments. Our attention is focused on the following phenomena: how do different cations modify the structure of the quartet? What is the stabilizing sequence of the monovalent cations for the quartet complexes?

Computational method by DFT

Selected distances and angles of the optimised structures were reported In Table 2 and Figure 1b.

Guanine. The guanine quartet (G-quartet) complexes with alkali cations are calculated at the B3LYP/6-31G(d,p) level of theory. The structures of the G-quartet complexes are depicted in Figure 3 for comparisons. These calculations predict an alkali ion interaction with the O6 atom and the (NH_2)-H...N7 and (N1)-H...O6 hydrogen bonds into the guanine quartet. After geometry optimisation, G-quartet complexes with metal ions are classified into different types of structures. A planar structure is obtained for Na^+-G-quartet complex (Figure 3b). The sodium ion occupies the central cavity within the plane of the guanine quartet. The guanine quartet adopts a plane Hoogsteen type base pairs geometry which is a square co-planar array of guanine bases associated through hydrogen bonds that involves N1, N7, O6 and N2 groups of each base (Figure 1b). In fact, Na^+-complex shows small deviations from the plane of the hydrogen-bonded system, the cation is not exactly located in the plane of the quartet, which is revealed by the (O6-Cat^+-O6') angle between opposite bases of about 174° (Figure 1b, Table 2). Moreover, guanine does not adopt exactly a C4 symetry, deviations are observed in hydrogen bond and cation base lengths. In fact, opposite guanine structures are analogous together but are slightly different from the adjacent bases (Table 2). In comparison with Na^+-complex, the other alkali cation complexes display a non-planar structure. With potassium, the G-quartet adopts a planar Hoogsteen type structure (within C4 symetry) but with the alkali cation located above the quartet plane as the cavity is too small for potassium cations. A distance of about 1.1 Å between K^+ (Figure 3c) and the root mean square plane of the guanine bases, is observed. Alternatively, the stricking observation, with the Li^+-complex (Figure 3a), is the change of G-quartet structure. The quartet adopts a sort of bifurcated hydrogen bond structure, where hydrogen atoms are located above and below the base plane in an alternating sequence, which prevents stacking of guanine bases. Obviously, this structure allows more close contacts between the bases and the lithium ion (Table 2). With this geometry, the contacts are similar but the distance (N1)-H...O6 is shortened whereas (NH_2)-H...N7 is lengthened.

Theoretical calculations determine the distance between atoms, which can be relied upon to strengthen the interactions in the cationized complex. Selected geometric parameters are listed in Table 2. The size of the cations strongly influences the structural parameters of the

cation-quartet complexes. The distances between the alkali cations and the O6 atom of the guanine bases are calculated to be 1.976 and 2.025 Å (distances reported for adjacent bases) for Li^+, 2.267 and 2.268 Å for Na^+ and 2.587 Å for K^+. Then, smaller cation attracts more strongly the base O6 atom. Alternatively, the distance O6...O6' between adjacent bases reflects the strengths of metal ion interaction. It increases from 2.944 and 2.976 Å (for two consecutive sides of the square containing the O6 atoms) in Li^+-complex to 3.202 and 3.203 Å in Na^+-complex and to 3.407 Å in K^+-complex. The change in the Cat^+...O6 bond length suggests that the nature of the alkali cation does also influence the hydrogen bonding inside the G-quartet. Above all, the hydrogen bond (N1)-H…O6 length should be modified by the nature of the alkali cation. The distances are 1.666 and 1.716 Å for Li^+, 1.766 Å for the Na^+-G-quartet and 1.865 Å for the K^+-G-quartet complexes. Additionally, the hydrogen of the amino group in guanine forms strong H-bonds with the N7 atoms of the other guanine (with a value of 1.906 and 2.023 Å with Li^+, 1.882 and 1.883 Å with Na^+ and 1.926 Å with K^+). The variation of (NH_2)-H…N7 H-bonds reflects the change of quartet structure from Li^+-complex to other alkali cations complexes.

Xanthine. Similarly to guanine optimized structures of xanthine quartet (X-quartet) complexes with the monovalent cations are determined and reported in Figure 4. In all cation complexes, the tetrameric form consists of four diketo tautomers of xanthine base with alkali ion interacting to base O6 atom. X-quartet complexes with alkali cations display different types of structures according to the cation size. Li^+-X-complex adopts a non-planar structure (Figure 4a). The X-quartet adopts a bifurcated hydrogen-bonded systems associated through one (N1)-H...N7 hydrogen bond of 1.716 Å . Lithium atom displays a tetrahedral geometry with an (O6-Cat^+-O6") angle between opposite bases of about 137.5°. In contrast, with Na^+ and K^+, the X-quartet displays analogous structures. Optimised structures of X-quartet display a Hoogsteen type structure stabilised by (N1)-H...O6 and (N9)-H...O2 hydrogen bonds (distances are listed in Table 2). The Na^+-complex (Figure 4b) shows a planar geometry (as for the guanine complex), where the sodium ion is nearly located in the central axis in the plane of the X-quartet [the angle (O6-Cat^+-O6') between opposite bases of 177.1°]. However, the quartet deviates slightly from a mean square structure as (O6-Cat^+-O6') angles between adjacent bases of 89.9° and 90.1° are calculated. Similarly to G-quartet, complexes of X-quartet with K^+ (Figure 4c) display a non-planar geometry as the cation is located outside of the X-quartet plane [with a distance of about 1.15 Å between K^+ and the quartet plane and the (O6-Cat^+-O6) angle between opposite bases of 130.3°]. The X-quartet adopts a Hoogsteen structure,

but not exactly a planar geometry in comparison with Na^+-complex or compared to G-quartet complexes. The quartet presents a more twisted structure where the (N1)H...O6 length is increased to 1.500 Å and the (N9)H...O2 hydrogen bond is strenghtened (1.484 Å) compared to Na^+-complex

Finally, large differences are observed between optimized structures of X-quartet complexes with the different alkali cations and it is straigthforward to correlate the calculated distances between atoms and the strength of interactions. We could conclude that stronger interactions are observed for smaller cations as it was already pointed with G-quartet. The distances between cations and the O6 atoms are calculated to be 1.795 Å for Li^+, 2.072 to 2.074 Å for Na^+ and 2.493 Å for K^+-X-complexes. Similarly, the distance O6...O6' between adjacent bases are shortened for Li^+ (see Table 2). However, direct comparison cannot be done on hydrogen bond lengths because of the different geometries observed for the alkali cation-X-quartet complexes (see Figure 4a-4c).

Moreover, among the various complex structures calculated by DFT, the reported structures for Na^+ and K^+ complexes in Figure 4d and 4e, are characterized by close energy levels as compared to their most stable forms, respectively. Note that for Li^+-complex, the other structures present a large energy difference and are not discussed. Both complexes noted 2Na (Figure 4d) and 2K (Figure 4e) present different structural features when compared to the most optimized structures. The 2Na complex displays a non planar geometry as the quartet present a twisted geometry with one (N1)-H…N7 hydrogen bond between each base of 1.757 Å . But the cation is located in the central cavity of the X-quartet with a tetrahedral geometry. The (O6-Cat^+-O6) angle between opposite bases and adjacent bases are calculated to be 152.9° and 93.1°, respectively. Thus, this structure is expected to be less stable although it is expected to have a stronger metal ion interaction (Cat^+…O6 length is slightly shortened to 2.057 Å). The 2K complex structure consists in four 2-enol-6-keto tautomers of xanthine associated through (N1)-H…O6 and (O2)-H…N7H-bonds of 1.524 and 1.613 Å , respectively, with a K^+ cation located outside from the plane of the X-quartet. The (O6-Cat^+-O6’ ’) angle between opposite bases and adjacent bases are calculated to be 123.3° (or 125.5°) and 77.5°, respectively. Such structures present a decreased Cat^+...O6 and O6...O6’ distances of 2.475 Å and 3.099 Å , respectively.

To give a clear picture of the quartet stability, energetic parameters describing the strength of interaction are calculated as the enthalpy of the following reaction: $xan_4 + Cat^+ \rightarrow [xan_4+Cat]^+$.

Finally, the binding sequence determined by calculations (Table 2) between the monovalent cations and the xanthine quartet follows the order $Li^+ > Na^+ > K^+$, a similar trend to that determined for guanine base.

DISCUSSION

We have demonstrated using ESI that guanine and xanthine preferentially form cationized tetrameric clusters with alkali cations. The existence of cationized clusters for both bases indicate that for systems bearing acceptor and donor groups, the cooperative effect between neighboring groups can enhance stabilisation of hydrogen bond systems. In contrast, the absence of large cationized clusters for hypoxanthine, is consistent to its structure. This behavior indicates that hydrogen bond to N7 to N2 or 02 for guanine and xanthine, respectively, is a determining factor in the stability of the cationized quartet. However, some cationized clusters observed (particularly for hypoxanthine) result from non-specific aggregation ionization during the ionization process[17,18,19]. Nevertheless, gas phase cation-stabilized tetrameric species for guanine exhibits similar behavior to that previously reported[25,29] for solution-phase guanosine quartet. It shows the ability of ESI ionization for transferring specific non-covalent interactions into the gas phase. However, the exact nature of the interactions between metal ions and nucleobases is not fully characterized. To complement experimental observations, DFT calculations were undergone. The most stable non planar structure for the Li^+-complex prevents the stacking of guanine quartets and is correlated by solution-phase studies which showed that Li^+ inhibits G-tetraplex formation. In contrast, both Na^+- and K^+-quartet complexes conformations consist of planar Hoogsteen type structure, with the cation either inside or just located above the quartet plane. These results are consistent with the solution-phase studies on quadruplex formation. Sodium and potassium are known to stabilize the guanosine quartet responsible for multistrand formation of telomeres[12,15]. Analogous structures have been already determined with previous DFT and HF calculations[13,14].

Similarly, gas phase experiments and DFT calculations were performed on xanthine. The structure displays two carbonyl groups, so various xanthine tautomeric forms can be implied in the hydrogen-bonded systems. Xanthine base pairing has been studied in linear PNA, and it was shown by circular dichroism that mixed diketo and dienol tautomers formed the most favored self-complementary base pairs[36]. In duplexes poly(xanthine) fibres, base are linked by

single hydrogen bonds N1..O6[37]. Furthermore, its structure is analogous to uracil pyrimidine base. Uracil (or even thymine) have been found to form tetrameric and pentameric magic number clusters[25,29] in the gas phase cationized by Na^+ and K^+, respectively. Moreover, the formation of uracil quartet has been demonstrated in solution[38]. Then, observation of magic number clusters for the xanthine with alkali cations was therefore expected. In the presence of these cations, tetrameric magic number complexes were observed under ESI-MS conditions. Moreover, abundant cationized octamer species were observed with potassium. Theoretical calculations demonstrated that the most stable xanthine quartet complex with lithium adopts a bifurcated non-planar structure, which can be correlated to the absence of cationized tetramers in the ESI experiments. Moreover, the most stable quartet in Na^+ and K^+-complexes cations form a stabilised planar and non-planar Hoogsteen structure, respectively. Such geometry for quartet complexes can explain the presence of abundant cationized tetramers in the gas phase. In comparison with similar guanine quartet complex, the optimized structures of the xanthine complexes show closer contacts between bases and alkali cations (see Table 2). Moreover, the hydrogen bonds between each xanthine bases are shorter than that observed in the quartet guanine. These results strongly suggest that the xanthine-cationized complexes should be more stable than the complex $[gua_4+Cat]^+$. Indeed, the hydrogen-bond symmetry between the bases [(N1)-H...O6 and (N7)-H...O2] in the cationized quartet of xanthine is consistent with this hypothesis.

DFT and HF studies[13,14] have revealed that the guanine and xanthine quartet conformations depend upon the alkali cation. Indeed, they are stabilised in the following order $Li^+ > Na^+ > K^+$, which is in contrast with the stabilizing order occurring in aqueous solution[12,15]. The preferential gas phase stabilization effect of Li^+ *versus* the other alkali metal ions is not reflected in the ESI experiments. In fact, the low abundance (or the absence) of the $[gua_4+Li]^+$ and $[xan_4+Li]^+$ cationized tetramers can be explained by the calculated twisted geometries. In previous solution-phase studies[12,15], some hypothesis have been proposed and the preferential stabilization effect of K^+ *versus* the other alkali cations in guanine and xanthine cationized tetramers has been explained by considering the potassium cation location between two quartets. Considering this hypothesis, large metaclusters as $[gua_8$ (or $xan)_8 + K]^+$ cationized octamers are predicted. Even if an abundant octamer adduct with K^+ was detected for xanthine (which is consistent with the existence of the sandwich-like structure) it was not observed for guanine bases (Figure 2). The complete lack of octamer complex with K^+ for guanine is an intriguing observation: it may be explained by experimental limitations, certainly

due to inadequate guanine concentration because of guanine poor solubility. Subsequently DFT calculations on cationized octamer of guanine and xanthine with K^+ were undertaken and reported in Figure 5. Calculations show that such systems are stabilized by chelation of cations with carbonyl groups and also a staking effect between bases. Furthermore, the octamer adduct with K^+ for the guanine (Figure 5a) presents a more twisted structure as compared to $[xan_8 + K]^+$ (Figure 5b). The xanthine octamer complex with potassium (Figure 5b) displays a nearly plane quartet (with cation located between both the quartet planes) which involve stronger stacking effect between both quartets as compared to $[gua_8 + K]^+$ (Figure 5a). From these findings, it is expected that the complex $[xan_8 + K]^+$ should be more stable than the complex $[gua_8+Cat]^+$ and could explain the preferential formation of stable xanthine octamer in the ESI experiments.

CONCLUSION

In spite of the poor solubility of the guanine base, its clusters with chloride salts were observed by ESI-MS and compared to the clustering of xanthine and hypoxanthine, bases that are structurally close to guanine. Finally; abundant cationized tetramers were detected for guanine and xanthine upon addition of Na^+ and K^+ cations. Observation of such magic number clusters reflects the presence of specific quartet complexes in solution. Such results support previous observations in solution in which G-quadruplexes in the telomeres are stabilized by K^+ or Na^+ cations. The complementary DFT study on the guanine and xanthine quartet complexes with three alkali cations has shown that the optimized cation-quartet complex structures display a significant change in the bond pattern of the quartet. The conformation of cation-complexes adopts the normal four-stranded Hoogsteen-bonded G-quartet structure or a more bifurcated hydrogen bonded system according to the alkali cation nature. The gas-phase binding sequence between the monovalent cations and the xanthine quartets follows the order $Li^+ > Na^+ > K^+$, which has been already determined for guanine quartet. However, this trend does not govern the ion selectivity of the guanine tetraplexes in solution. In fact, this apparent contradiction can be explained by the observation of octamer adduct with K^+ for xanthine but not with guanine. Both geometric parameters and stabilization energies of the different cation-complexes indicate that the best hypothesis for octamer formation is a "sandwich" form which is consistent with the preferential stabilizing effect of the K^+ in solution. This absence of

guanine metaclusters should be explained by guanine’ s poor solubility in aqueous solution as compared to xanthine.

Captions

Figure 1: Structures of (a) nucleobases studied and (b) G-quartet.

Figure 2: Mass spectra of (a) guanine and (b) xanthine with addition of K^+.

Figure 3: Structure of the guanine quartet cationized with (a) Li^+, (b) Na^+ and (c) K^+. Optimization has been made at the B3LYP/6-31G* level of theory.

Figure 4: (I) Structure of the guanine quartet cationized with (a) Li^+, (b) Na^+ and (c) K^+. Optimization has been made at the B3LYP/6-31G* level of theory. (II) Structures and energy ($kJ.mol^{-1}$) determined for (d) Na^+-complex called 2Na and (d) K^+-complex called 2K (in comparison with their most form Na^+-complex E(1Na)= -2368.07572 $kJ.mol^{-1}$ and K^+-complex E(1K)= -2801.27193 $kJ.mol^{-1}$, respectively).

Figure 5: Structure of the (a) guanine and (b) xanthine octamer cationized with K^+. Optimization has been made at the B3LYP/6-31G* level of theory.

Table 1: Clusters of nucleobases formed under ESI conditions in the presence of protons and lithium, sodium or potassium cations with their normalized abundances.

[I] Cation adduct with the normalized abundance given in parentheses, where the base peak is set to be 100%. [ii] Magic number clusters, unusually stable clusters compared with their neighbors, are marked in bold.

Table 2 : Selected distances and angles of (a) guanine and (b) xanthine-quartet complexes.

Note that two set of values are reported because opposite guanine structures are analogous together but are slightly different from the adjacent bases

	acidified	Li^+	Na^+	K^+
Guanine	M_1 (100) [i]	M_1 (100)	M_1 (100)	M_1 (100)
	M_2 (29)	M_2 (49)	M_2 (66)	M_2 (51)
	M_3 (15)	M_3 (8)	M_3 (2)	M_3 (6)
		M_4 (18) [ii]	M_4 (36)	M_4 (30)
Xanthine	-	M_1 (100)	M_1 (100)	M_1 (100)
		M_2 (39)	M_2 (38)	M_2 (55)
		M_3 (19)	M_3 (26)	M_3 (35)
			M_4 (75)	M_4 (64)
				M_8 (81)
Hypoxanthine	-	M_1 (100)	M_1 (100)	M_1 (100)
		M_2 (63)	M_2 (80)	M_2 (86)
		M_3 (7)		

Table1

(a) Bonds (in Å)	$[gua_4+Li]^+$	$[gua_4+Na]^+$	$[gua_4+K]^+$
Rions	0.68	0.97	1.33
Cat^+ …O6	1.976-2.025*	2.267-2.268*	2.587
O6…O6' (between adjacent bases)	2.944-2.976*	3.202-3.203*	3.407
H-bond (N1)H…O6	1.666-1.716*	1.766	1.865
H-bond (N2H)H… N_7	2.023-1.906*	1.882-1.883*	1.926
Angles (in °)			
O6-Cat^+-O6' (adjacent bases)	94.7-96.1*	89.8	82.3
O6-Cat^+-O6' ' (opposite bases)	137.7-149.6*	173.9-174.3*	137.2

(b) Bonds (in Å)	$[xan_4+Li]^+$	$[xan_4+Na]^+$	$[xan_4+K]^+$
Cat^+…O6	1.795	2.072-2.074	2.493
O6-O6' (between adjacent bases)	2.700	2.930	3.200
H-bond (N1)H…O6	Only (N1)H…N7 of 1.716	1.480-1.482	1.558
H-bond (N9)H…O2		1.496-1.497	1.484
Angles (in °)			
O6-Cat^+-O6' (adjacent bases)	97.5	89.9-90.1	79.8

O6-Cat^{+}-O6’ ’ (opposite bases)	137.5	177.1	130.3
4xan + Cat^{+} $\rightarrow$ $[4Xan+Cat]^{+}$ (Δ H (Cat^{+}) in $kJ.mol^{-1}$)	- 1055	- 719	- 644

Table2

(a)

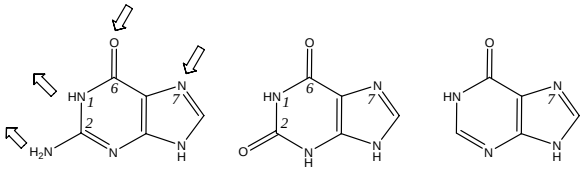

(b)

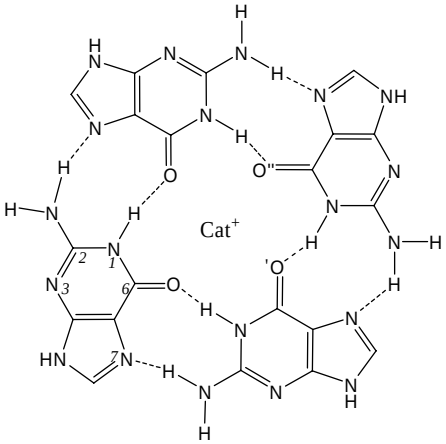

Figure 1

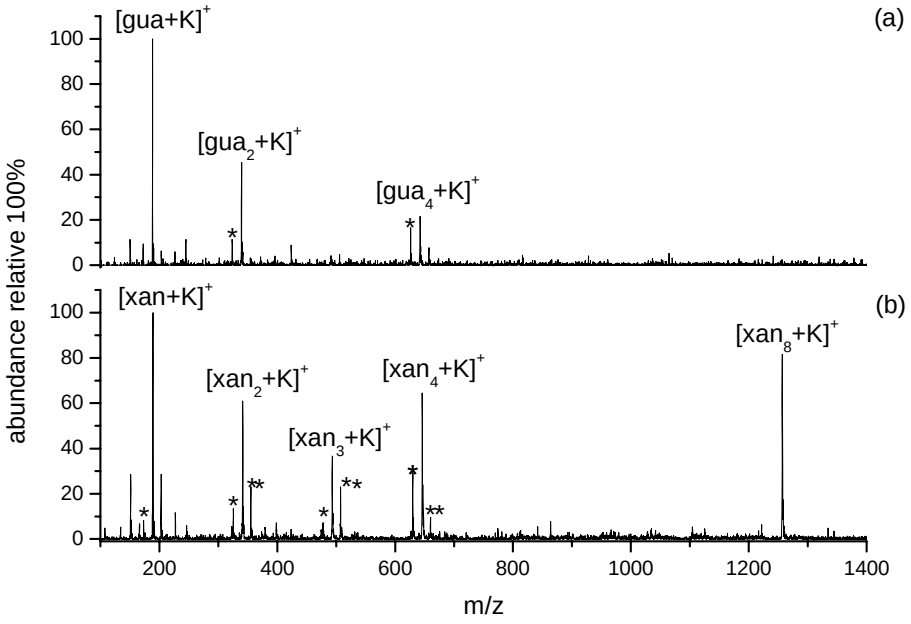
[gua+K]+
(a)
100
80
60
40
20
0
[gua2+K]+
[gua4+K]+
*
*
[xan+K]+
(b)
[xan8+K]+
[xan2+K]+
[xan4+K]+
[xan3+K]+
abundance relative 100%
200
400
600
800
1000
1200
1400
m/z

Figure 2

(a) $[gua_4+Li]^+$ (b) $[gua_4+Na]^+$ (c) $[gua_4+ K]^+$

Top View

Side View

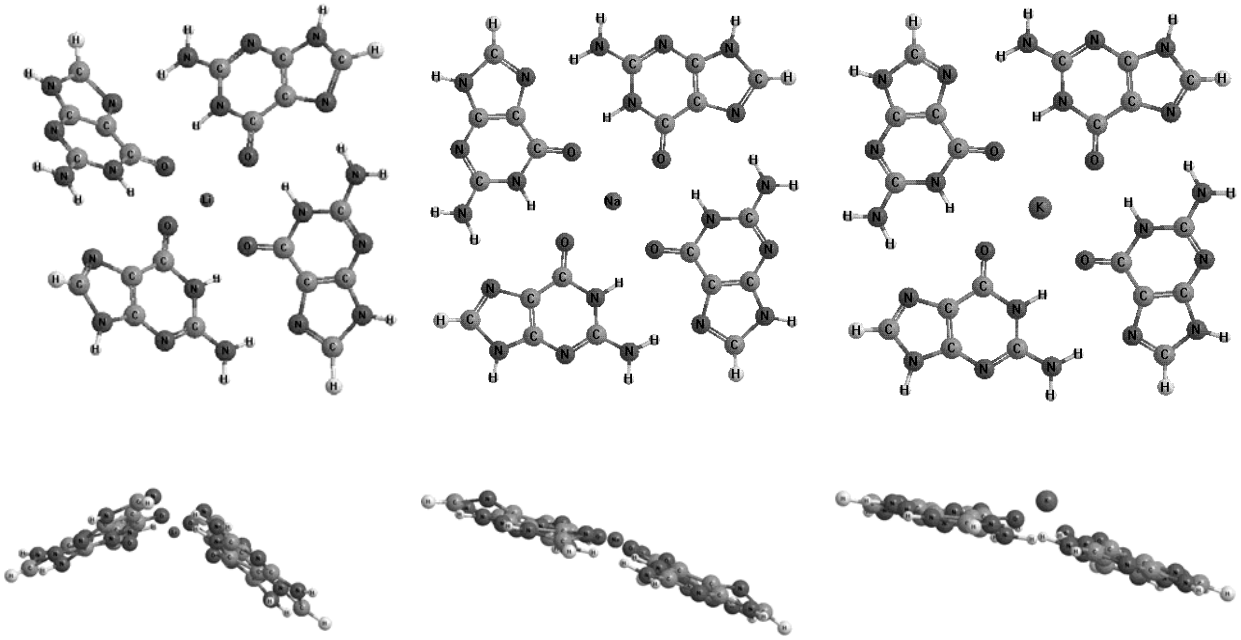

Figure 3

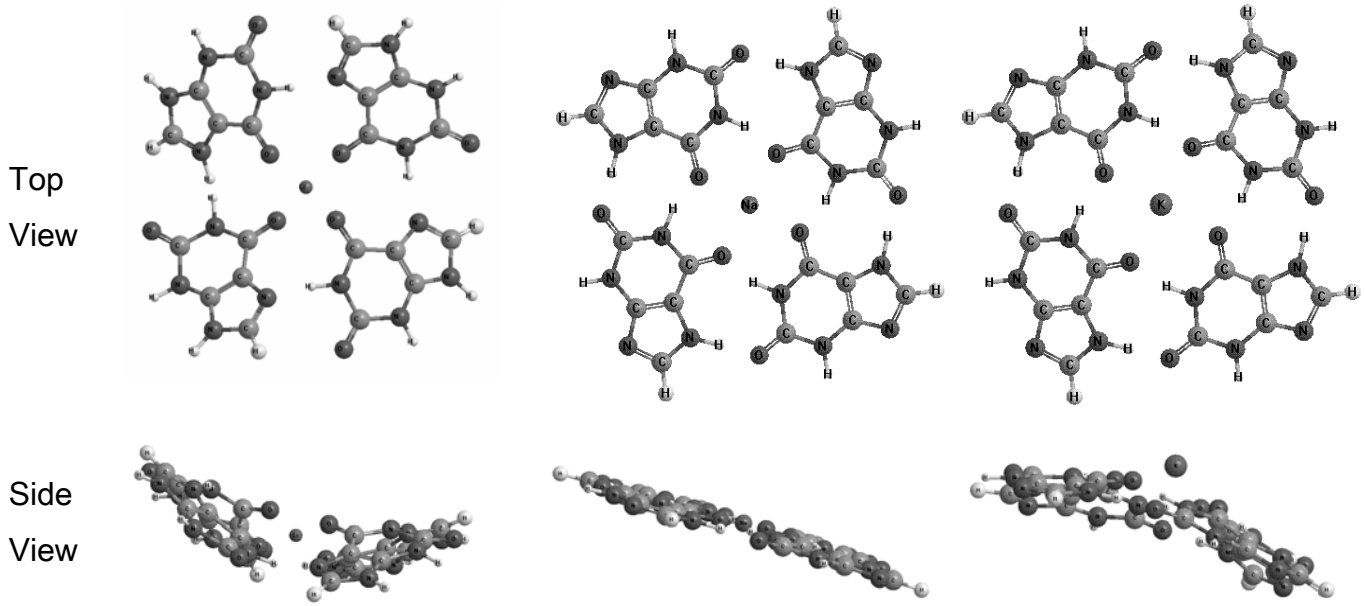
I
(a) [xan4+Li]+
(b) [xan4+Na]+
(c) [xan4+K]+
Top View
Side View
II
(d) 2Na
ΔE= 15 kJ.mol-1
(e) 2K
ΔE= 37 kJ.mol-1
Top View
Side View

Figure 4

(a) $[gua_8+K]^+$

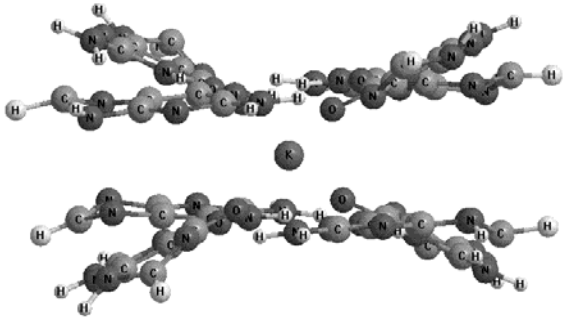

(b) $[xan_8+K]^+$

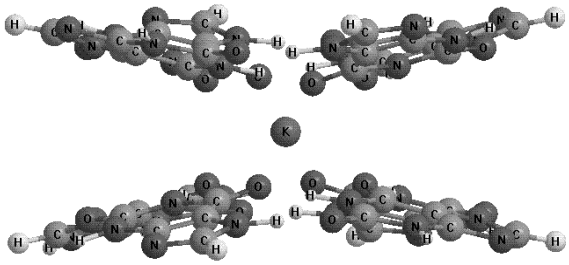

Figure 5

REFERENCES

[1] Neidle S, Parkinson G.N. *Current Op. Struct. Biol.* 2003; 13(3): 275
[2] Rezler E.V, Bearss D.J, Hurley L.H. *Annu. Rev. Pharmacol. Toxicol.* 2003; 43: 359
[3] Hsu Y.H, Lin, J.J. *Acta Pharmacologica Sinica.* 2005 ; 26 (5): 513
[4] Williamson, J.R, Raghuraman, M.K. Cech T.R. *Cell.* 1989*;* 59 (5): 871
[5] Takeda K, Noguchi, K., Shi, W. *Proc Natl Acad Sci USA.* 1997; 94: 3801
[6] Wegenka U.M, Lutticken, C, Bushmann. J. *Mol Cell Biol.* 1994; 14*:* 3186
[7] Otero R, Schöck, M., Molina, L.M., Lægsgaard, E. , Stensgaard, I. , Hammer, B. , Besenbacher, F.; *Angewandte Chemie International Edition*. 2005; *44 (15)*: 2270
[8] Daniele, P.G., Prenesti, E., Berto, S., Zelano, V. , Aruga, R. *Annali di Chimica*. 2004; *94 (3)*: 229
9 Bromberg, J., Darnell J.E. Oncogene. 2000; 19: 2468
10 Eline M. Basilio Janke, Anita Dunger, Hans-Heinrich Limbach, Klaus Weisz, Magnetic Resonance in Chemistry, Volume 39, Issue S1, Date: December 2001; Pages: S177-S182
[11] Kaucher M.S., Lam, Y.-F., Pieraccini, S., Gottarelli, G., Davis, J.T. *Chem.-Euro. J.* 2004; *11 (1)*: 164
[12] Hud, N.V. Smith, F.W. Anet,A.L. Feigon, J. *Biochem*. 1996; 35: 15383
[13] Gu, J., Leszczynski J., *J. Phys. Chem. A* 2000; *104*: 6308
[14] Meyer, M., Steinke, M. Brandl, *J. Computational Chemistry*, 2001; *22(1)*: 109
[15] Ross, W.S. Hardlin, C.C. *J. Am. Chem. Soc.* 1994; 116: 6070
[16] Fenn, J. B.; Mann, M., Meng, C. K., Wong, S. F., Whitehouse C. M. *Science* 1989; *246*: 64
[17] Loo, J.A., *Mass Spectrom. Rev*. 1997; *16 (1)*: 1
[18] Wang, G., Cole, R.B. , *Anal. Chem*. 1998; *70*: 873
[19] Nemes, P, Schlosser, G, Vékey, K, *J. Mass Spectrom.* 2005; *40*: 43
[20] Triolo, A., Arcamone, F.M.; Raffaelli, A., Salvadori, P. *J. Mass Spectrom.* 1997; *32 (11)*: 1186
[21] Goodlett DR , Camp DG , Hardin CC, Corregan M, Smith RD. *Biol Mass Spectrom*. 1993; *22*: 181
[22] Manet I, Francini L, Masiero S, Pieracini S, Spada GP, Gottarelli G. *Chim. Acta.* 2001; *84*: 2096
[23] Baker, E.S. , Bernstein, S.L. ; Bowers, M.T. *J.Am. Soc. Mass Spectrom. 2005; 16: 989*
[24] Gabelica, V., Rosu, F.; Witt, M. , Baykut, G. ; De Pauw, E. *Rapid. Commun. Mass Spectrom.* 2005; *19*: 201
[25] Manet, I. Francini, L. Masiero, S. Pieraccini, S. Spada, G.P. Gottarelli, G. *Helvetica Chimica Acta* 2001; 84: 2096
[26] Koch, K.J., Aggerholm, T., Nanita, S.C.; Cooks, R.G. *J. Mass Spectrom*. 2002; *37*: 676
[27] Sakamoto, S., Nakatani, K.; Saito, I., Yamaguchi, K. *Chem. Commm*. 2003; 788
[28] Moriwaki, H. *J. Mass Spectrom*. 2003; *38*: 321
[29] Aggerholm, T., Nanita, S.C., Koch, K.J., Cooks R.G. *J. Mass Spectrom*. 2003; *38*: 87
[30] Kukushima, K., Iwahashi, H. *Chem. Commm*. 2000; 895
[31] Baker, A.S, Gidden, J., Ferzoco, A., Bowers M.T. *Phys. Chem. Chem. Phys.* 2004; *6*: 2786
[32] Hypoxanthine and xanthine are not incorporated into the biological nucleic acids but are important intermediates in the synthesis and degradation of the purine nucleotides
[33] Strittmater, E.F , Williams, E.R. *Int. J. Mass Spectrom.*2001; *212*: 287
[34] Pepe, C. Rochut, S. Pommard, J.P. Tabet, J.C. *Rapid Com. Mass Spectrom*. 2004; 18: 307
[35] Frisch MJ, Trucks GW, Schlegel HB, Scuseria GE, Robb MA, Cheeseman JR, Zakrzewski VG, Montgomery JA, Stratmann Jr RE, Burant JC, Dapprich S, Millam JM, Daniels AD, Kudin KN, Strain MC, Farkas O, Tomasi J, Barone V, Cossi M, Cammi R, Mennucci B, Pomelli C, Adamo C, Clifford S, Ochterski J, Petersson GA, Ayala PY, Cui Q, Morokuma K, Rega N, Salvador P, Dannenberg JJ, Malick DK, Rabuck AD, Raghavachari K, Foresman JB, Cioslowski J, Ortiz JV, Baboul AG, Stefanov BB, Liu G, Liashenko A, Piskorz P, Komaromi I, Gomperts R, Martin RL, Fox DJ, Keith T, Al-Laham MA, Peng CY, Nanayakkara A, Challacombe M, Gill PMW, Johnson B, Chen W, Wong MW, Andres JL, Gonzalez C, Head-Gordon M, Replogle ES, Pople JA. *Gaussian 98 (Revision A.7).* Gaussian, Inc., Pittsburgh PA, 2002.
[36] Hoffmann, M.F.H. Brückner, A.M. Hupp, T. Engels, B. Diederichsen, U. *Helvetica Chimica Acta*, 2000; 83: 2580
[37] Kulikowska, E, Kierdaszik, B, Shugar, D. *Acta Biochimica Polonica*, 2004; 51 (2): 493
[38] Cheong, C, Moore, P.B. *Biochemistry*, 1992; 31: 8406